

Article

Spatial and Temporal Changes of Urban Built-Up Area in the Yellow River Basin from Nighttime Light Data

Jingxu Wang ¹, Shike Qiu ¹, Jun Du ¹, Shengwang Meng ^{2,*}, Chao Wang ¹, Fei Teng ¹ and Yangyang Liu ³

- ¹ Key Laboratory of Remote Sensing and Geographic Information System of Henan Province, Institute of Geography, Henan Academy of Sciences, Zhengzhou 450052, China; jingxuwang-2020@igs-has.cn (J.W.); qiushike@igs-has.cn (S.Q.); dujun@igs-has.cn (J.D.); wangchao@igs-has.cn (C.W.); tengfei@igs-has.cn (F.T.)
- ² Qianyanzhou Ecological Research Station, Key Laboratory of Ecosystem Network Observation and Modeling, Institute of Geographic Sciences and Natural Resources Research, Chinese Academy of Sciences, Beijing 100101, China
- ³ PIESAT International Information Technology Limited, Beijing 100195, China; liuyangyang_yf@piesat.cn
- * Correspondence: mengsw@igsnr.ac.cn; Tel.: +86-010-6488-9913

Abstract: Nighttime light (NTL) images obtained by the Visible Infrared Imaging Radiometer (VIIRS) mounted on the National Polar-orbiting Partnership (NPP) could objectively represent human activities and instantly identify urban shapes on a temporal and spatial scale. From 2013 to 2020, the built-up areas of eight provincial capital cities were extracted using NPP/VIIRS NTL data to examine the dynamic changes in city expansion and socioeconomic development in the Yellow River Basin during the urbanization process. The spatial characteristics of urban built-up area expansion were generated using the eight-quadrant analysis method and combined with the statistical data of population and (gross domestic product) GDP to analyze the correlations between the light intensity of built-up areas, population and GDP; this enables an understanding of the changes in population and economy in the development of urban built-up area expansion. The findings show that: (1) unbalanced city development existed in the Yellow River Basin's upper, middle, and lower reaches, and the expansion and light intensity of cities in the upper reaches were slower than those in the middle and lower reaches; (2) the spatial differentiation of urban expansion was significant between each of the reaches in the Yellow River Basin, and greatly influenced by natural geographical elements; and (3) positive correlation exists between light intensity, population, and GDP in the built-up areas of the middle and lower reaches, while the correlations in the upper reaches were not stable. In conclusion, light data indirectly reflects urban development and could be used as a substitute variable for socioeconomic development indicators under certain conditions.



Citation: Wang, J.; Qiu, S.; Du, J.; Meng, S.; Wang, C.; Teng, F.; Liu, Y. Spatial and Temporal Changes of Urban Built-Up Area in the Yellow River Basin from Nighttime Light Data. *Land* **2022**, *11*, 1067. <https://doi.org/10.3390/land11071067>

Academic Editor: Kai Fang

Received: 16 June 2022

Accepted: 11 July 2022

Published: 13 July 2022

Publisher's Note: MDPI stays neutral with regard to jurisdictional claims in published maps and institutional affiliations.



Copyright: © 2022 by the authors. Licensee MDPI, Basel, Switzerland. This article is an open access article distributed under the terms and conditions of the Creative Commons Attribution (CC BY) license (<https://creativecommons.org/licenses/by/4.0/>).

Keywords: urban expansion; nighttime light; light intensity; socioeconomic development; Yellow River Basin

1. Introduction

China's rapid growth and the regular flow of domestic socioeconomic and population factors have accelerated the urbanization process in the Yellow River Basin in recent years [1,2]. However, it has also brought increasing pressure and challenges to the protection of the ecological environment [2]. The natural ecological land around cities and towns has been encroached upon by humans as a result of the continual expansion of urban land exacerbating the land shortage. This situation will cause the degradation of the ecological environment, resource shortages, the pollution of soil, air, and water, and other problems [3–5]. In 2019, "ecological protection and high-quality development in the Yellow River Basin" was incorporated into the national strategy by the government for regional coordination [6]. This national strategy was designed to reduce the ecological conflict between urbanization and natural space; also to explore the ecological priority and green development to promote green urbanization and ecological protection in the Yellow River

Basin [4]. Therefore, clarifying the relationship between the characteristics of spatial and temporal changes throughout the urban expansion and socioeconomic, demographic, and physical geographical environment is thus critical for the future qualitative development of cities of Yellow River Basin [1,7].

The emergence of Remote Sensing information technology has made it possible to monitor the built-up area change accurately and rapidly for estimating the urbanization process. Remote sensing data in the form of nighttime light (NTL) provide a consistent and independent measurement of urban built-up areas [8]. The NTL images are formed by detected light radiation induced by human activities on the earth's surface, and they can directly reflect artificial surface regions and locations with significant human activity [9,10]. The most often utilized long-term NTL data sources in recent years have been Defense Meteorological Satellite Program/Operational Linescan System (DMSP/OLS) data and Visible Infrared Imaging Radiometer Suite with National Polar-orbiting Partnership (VIIRS/NPP) data. Since the DMSP/OLS nighttime light images were no longer updated after 2013, NPP/VIIRS images with higher spatial resolution have been the most extensively used [11], and many researchers have demonstrated that NPP/VIIRS data have higher spatial accuracies than DMSP/OLS data for extracting built-up urban areas [12]. The study areas and application fields of remotely sensed NTL data, which are extremely objective and convenient, have substantially increased with the increasing number of data products [13–15]. NTL data have been found to have a widespread application in sectors such as urban expansion [9,16,17], social economy, and demographic data modeling and spatialization [18,19].

NTL data are targeted and may be utilized for rapid identification of urban forms and extraction of urban boundaries at spatial and temporal scales, as well as a complete analysis of urban spatial forms and expansion in urban development [20–22]. The extraction results of urban built-up regions have become more accurate as the application of NTL data in urban expansion and spatial structure analysis has matured [23]. At present, the threshold approach [23], mutation detection method [24], and spatial comparison method based on auxiliary information [15] are the most commonly used methods for extracting urban spatial patterns. For example, Milesi et al. [13] employed land use classification data to estimate DN thresholds of NTL images, from which urban boundary areas in the southeastern United States were extracted. Su et al. [15] have also demonstrated the applicability of NTL data for extracting the built-up regions in the Pearl River Delta with four periods of DMSP/OLS data between 1996 and 2005. Zheng et al. [9] have incorporated temporal information from the VIIRS time series and produced monthly maps of built-up areas of 30 global megacities to disentangle urban land changes into five categories.

Furthermore, except for the boundary change detection of urban expansion, NTL data has also been utilized to monitor the socioeconomic and human activities as a result of urban expansion [25]. Valuable studies have shown that NTL data have a positive relationship with socioeconomic development indicators such as population, gross national product (GNP), and gross domestic product (GDP) [26,27]. With the help of that good correlation, traditional population and GDP statistics data based on administrative districts can be spatialized to more intuitively depict the scale and distribution characteristics of both, which is useful for fine management and information-based city construction, as well as a better study of regional sustainable development [28,29]. However, some researchers have demonstrated that the use of light intensity in urban expansion and socioeconomic development should be implemented with limited or specific conditions, because of the unstable relationship between light intensity and socioeconomic development factors in different regions [30]. Therefore, this relationship should be reanalyzed in the upper, middle, and lower reaches of the Yellow River Basin that have a regional disparity in economic development.

Due to the sufficient satellite imagery data of long-time series NTL data and a lack of computing resources, the urban expansion detection methods and algorithms have not been applied in practice at a large scale. The Google Earth Engine (GEE) cloud platform is

an integrated platform for remote sensing and geographic information data processing [31]; it centralizes cloud computing services for data analysis and consists of petabytes of geospatial data, including full NTL archive data and algorithms for image processing with a JavaScript, Python-based API [32,33]. In this paper, we transferred the annual NPP-VIIRS NTL satellite images from the GEE platform with JavaScript as the data source to analyze the evolution of urban expansion of provincial capitals in the Yellow River Basin. The range of built-up areas of provincial capitals from 2013 to 2020 was obtained by using the OTSU algorithm from NTL images. The quadrant analysis method was used to examine the geographical and temporal change characteristics of provincial capital urban expansion. The aspects of socio-economic development in the urban expansion were addressed, taking into account indices such as population and GDP.

2. Study Area

The Yellow River rises in the central Qinghai Province and flows through nine provinces (Qinghai, Sichuan, Gansu, Ningxia, Inner Mongolia, Shaanxi, Shanxi, Henan, and Shandong) before joining the Bohai Sea near Kenli County and Dongying City (Figure 1). The mainstream of the Yellow River stretches over 5734 km, with a 4480 m elevation reduction between west and east. The Yellow River Basin is approximately 1900 km long from west to east and around 1100 km wide from north to south, with a watershed area of 795,000 km². The huge Yellow River Basin is high in the west and low in the east, with large height disparities along the west–east direction, noticeable climate change, and significant regional seasonal differences within the watershed. Annual precipitation in the basin decreases from southeast to northwest and is distributed relatively irregularly throughout the year. The Yellow River Basin stretches across three major economic zones in eastern, central, and western China, and the 69 cities within it differ substantially in terms of economic growth. The provincial capitals in the Yellow River Basin are regional political and economic centers, and their economic and social development is highly indicative of, and has a radiating influence on, the provinces' regional economic and social development. As a result, this study considered eight provincial capitals (except Chengdu) in the basin for analysis (Table 1) and used the NPP/VIIRS night-light photos from 2013 to 2020 to analyze the pattern changes in the built-up areas of each province's capital city.

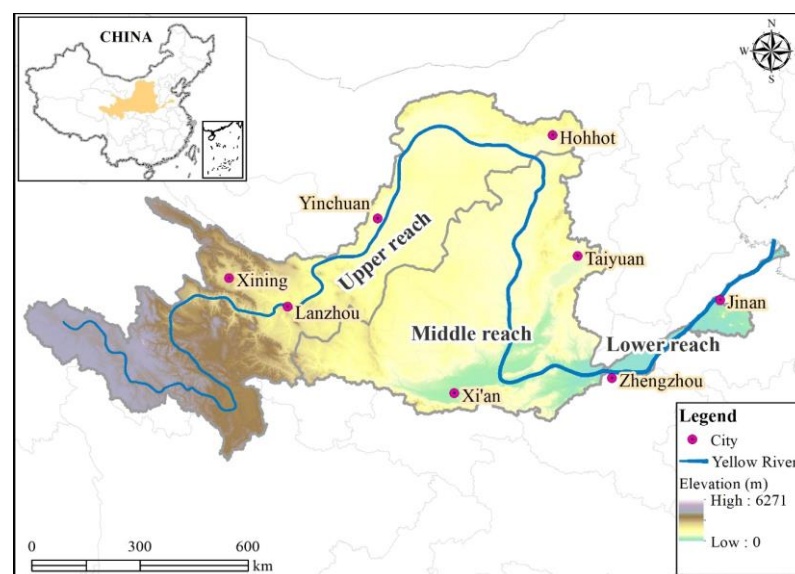


Figure 1. The study area of Yellow River Basin.

Table 1. The districts of each provincial capital in the Yellow River Basin.

	City	DEM (m)	Slop (°)	District
Upper reach	Xining	2237.72	10.10	Chengbei, Chengxi, Chengdong, Chengzhong
	Yinchuan	1517.42	10.46	Xixia, Jinfeng, Xingqing
	Lanzhou	1069.55	4.44	Xigu, Anning, Chengguan, Qilihe
	Hohhot	1035.55	3.83	Xincheng, Huimin, Yuquan, Saihan
Middle reach	Taiyuan	783.78	6.32	Jiancaoping, Wanbailin, Jinyuan, Xiaodian, Xinghualing, Yingze
	Xi'an	378.60	5.54	Weiyang, Lianhu, Yanta, Beilin, Baqiao, Xincheng, Chang'an, E'yi, Lintong, Yanliang, Gaoling
	Zhengzhou	83.54	4.40	Huiji, Jinshui, Zhongyuan, Guancheng Hui, Erqi
Lower reach	Jinan	68.22	8.16	Lixia, Tianqiao, Huiyin, Shizhong, Licheng, Changqing, Jiyang, Zhangqiu

3. Data Sources and Methods

3.1. NPP/VIIRS NTL Remote Sensing Images

The VIIRS is an essential sensor operated by the National Polar-orbiting Partnership satellite (Suomi NPP). The NPP satellite sensor has a 3000 km sweep width, traverses the equator every four hours, and has a spatial resolution of around 500 m in $nW\text{-cm}^{-2}\text{-sr}^{-1}$. Because the VIIRS Day/Night Band has a powerful nighttime weak light detection capacity and can identify faint surface lights, it is extremely useful for monitoring the earth's surface brightness at night. The brightness values in NPP/VIIRS photos are used to quantify light intensity, and the NTL data obtained comprised annual and monthly composite images, with radiance values less than 0 indicating no light. In this study, we apply the mean composite approach to generate the annual composite NTL image using monthly NPP/VIIRS composite NTL data from 2013 to 2020. The light intensity images of the administrative boundaries of each city were masked by light intensity thresholds and exported to extract the built-up boundaries. Figure 2 shows an example of the light intensity of the built-up area of Zhengzhou from 2013 to 2020.

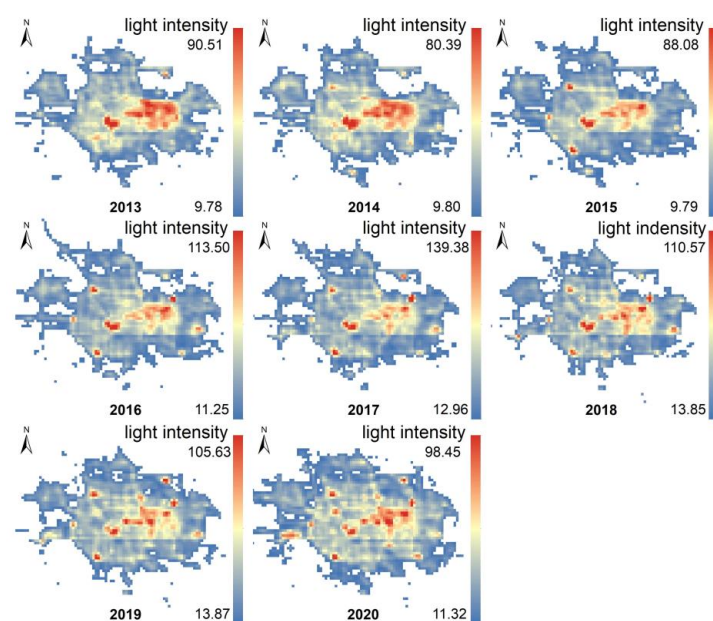


Figure 2. The light intensity of the built-up area of Zhengzhou city masked by light intensity thresholds from 2013 to 2020.

3.2. Basic Data

3.2.1. The Validation Data of Land Use

The validation data for extracting the urban built-up area boundary came from the land use/cover data set's artificial surface and impermeable layer. The land use/cover data for the Yellow River Basin in 2015 and 2017 were obtained from Prof. Gong Peng of Tsinghua University's GlobeLand30 dataset FROM-GLC (<http://data.ess.tsinghua.edu.cn/>, accessed on 13 May 2021) [34]. The Yellow River Basin land use classification in 2020 was derived from GlobeLand30 land cover classification data (<http://www.globallandcover.com/>, accessed on 27 May 2020) [35]. Because the urban built-up area is mostly made up of artificial surfaces like buildings, streets, and impervious layers, the impervious layer data from the 2015 and 2017 FROM-GLC datasets, as well as the artificial surface data from the 2020 GlobeLand30 V2020 surface cover type, were extracted as validation data to validate the built-up area boundary results.

3.2.2. Socioeconomic Statistics

GDP and population of the urban areas of the Yellow River Basin's capital cities were utilized as statistical indicators of socioeconomic development, and data were acquired from each city's statistical yearbooks from 2014 to 2020. Given the data delay in statistical yearbooks, where the data issued in a given year are the statistics from the previous year, the provinces' statistical yearbooks for 2021 have yet to be produced. As a result, statistical data from 2013 to 2019 were used to examine the relationship between socioeconomic development indicators and urban expansion characteristics.

3.3. Research Methodology

3.3.1. Light Threshold Extraction Using OTSU Thresholding Technique

To classify the NTL data, the threshold segmentation technique was employed for urban built-up area boundary extraction. NTL pixels that are greater than the given light threshold are classified as built-up areas, whereas NTL pixels that are lower than the light threshold are classified as unbuilt-up areas. The OTSU algorithm was utilized for threshold segmentation, which can be easily updated and employed in GEE to obtain light thresholds for urban boundary extraction.

The OTSU algorithm is used to calculate the following: if an image comprises N pixels, the grayscale value range is $[0, L - 1]$, the number of grayscale pixels i is n_i , and the probability of occurrence of each grayscale pixel is P_i , then: $P_i = n_i/N$, ($i = 0, 1, 2, 3, \dots, L - 1$), $\sum_{i=0}^{L-1} P_i = 1$. Using the threshold t , the image is separated into background pixel C_0 and object pixel C_1 . C_0 consists of pixels that have grayscale values of $[0, t]$, whereas C_1 is made up of pixels that have grayscale values of $[t + 1, L - 1]$. The likelihood of occurrence of any grayscale is $\mu_t = \sum_{i=0}^{L-1} iP_i$, and the probabilities of occurrence of C_0 and C_1 pixels are $\omega_0 = \sum_{i=0}^t P_i$ and $\omega_1 = \sum_{i=t+1}^{L-1} P_i = 1 - \omega_0$, and the average grayscale is $\mu_0 = \sum_{i=0}^t iP_i/\omega_0$ and $\mu_1 = \sum_{i=t+1}^{L-1} iP_i/\omega_1$; thus, $\mu_t = \omega_0\mu_0 + \omega_1\mu_1$. The interclass variance is defined as $\delta_t^2 = \omega_0(\mu_0 - \mu_t)^2 + \omega_1(\mu_1 - \mu_t)^2 = \omega_0\omega_1(\mu_0 - \mu_1)^2$, so that t takes values in the interval $[0, L - 1]$ and the t corresponding to maximum δ_t^2 is the optimal threshold to separate the two classes of pixels [36].

3.3.2. Quadrant Analysis

The quadrant analysis method was used to analyze the spatial differentiation of cities in the Yellow River Basin, starting with the geometric center of the extracted urban built-up area and dividing the built-up area into 8 quadrants (N, EN, E, ES, S, WS, W, and WN) for statistics of light intensity, slope, and urban expansion area, etc. in each quadrant, and then

the spatial expansion differences between cities in different periods, different directions and different elements were compared and analyzed to reflect the dominant direction and driving factors of the spatial and temporal changes of urban expansion.

3.3.3. Analysis of Urban Spatial Expansion

Urban spatial expansion is characterized by urban land expansion, the rate of expansion and the intensity of expansion are the characteristics of urban spatial expansion.

The expansion rate is the average yearly growth rate of an urban area during a given period, reflecting the absolute difference in the urban area's expansion speed per unit time. The calculating formula is:

$$V = \Delta U / \Delta t \times 100 \quad (1)$$

where V is the expansion rate; ΔU is the urban expansion area; Δt is the time span.

The expansion intensity N is the annual expansion ratio of the built-up area in a certain period relative to the built-up area in the baseline year, which represents the relative difference in the built-up area's expansion speed throughout that time horizon.

$$N = \Delta U / \Delta t / M \times 100 \quad (2)$$

where N is the intensity of urban expansion and M is the built-up area in the baseline year.

4. Result

4.1. Evaluation of the Accuracy of Urban Built-Up Area Extraction

The mean value approach was utilized in GEE to generate annual composite NTL images from 2013 to 2020, and the OTSU algorithm was used to compute light thresholds for built-up regions in cities in the Yellow River Basin in different years. Because of the Yellow River Basin's large spatial span, the light characteristics of different regions in different years are affected differently by climate and human activity images, so the light thresholds of urban built-up areas were calculated by region and year to extract the urban built-up area boundaries. The NTL results of the built-up region of each provincial capital city derived using the OTSU technique were validated using impervious layer and man-made surface data (LUCC) from ground cover categorization data from 2015, 2017, and 2020 (Figure 3). The NTL extraction results correlate well with the LUCC data, with R values larger than 0.8. The results show that the built-up areas retrieved in the GEE using the OTSU algorithm are highly accurate and may be used to study the expansion pattern of urban built-up regions.

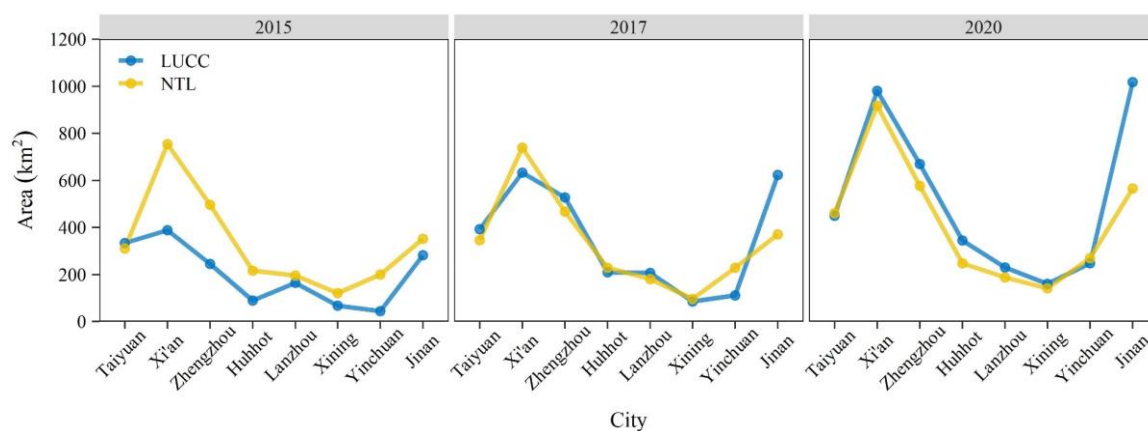


Figure 3. Verification of urban built-up areas extracted from NTL using impervious layers in LUCC data.

4.2. Temporal Characteristics of Urban Built-Up Area Expansion in the Yellow River Basin

The built-up areas of cities from 2014 to 2020 were superimposed onto the built-up areas in 2013, and the quadrant analysis method was used to divide the built-up areas of provincial capitals into equal sectors to objectively reflect the dynamic change characteristics of urban built-up area expansion in the Yellow River Basin (Figure 4). From 2013 to 2020, the built-up areas of cities in the upper, middle, and lower parts of the Yellow River Basin increased yearly and expanded outward surrounding each city’s historic urban centers, resulting in varied spatial form features of built-up areas (Table 2). The built-up area, AREA, and expansion rate V of cities in the upper Yellow River Basin (Lanzhou, Hohhot, Xining, and Yinchuan) are significantly smaller than those of cities in the middle and lower Yellow River Basins (Xi’an, Zhengzhou, Taiyuan, and Jinan), but among the upper river basin cities as Yinchuan and Xining outperform the middle river cities as Zhengzhou and Xi’an. Lanzhou, an important central city in Gansu Province, has a decreasing rate of urban built-up area increase. Jinan, the final major city downstream of the Yellow River Basin, has the highest expansion rate V and expansion intensity N of any city, at 28.95% and 9.31%, respectively.

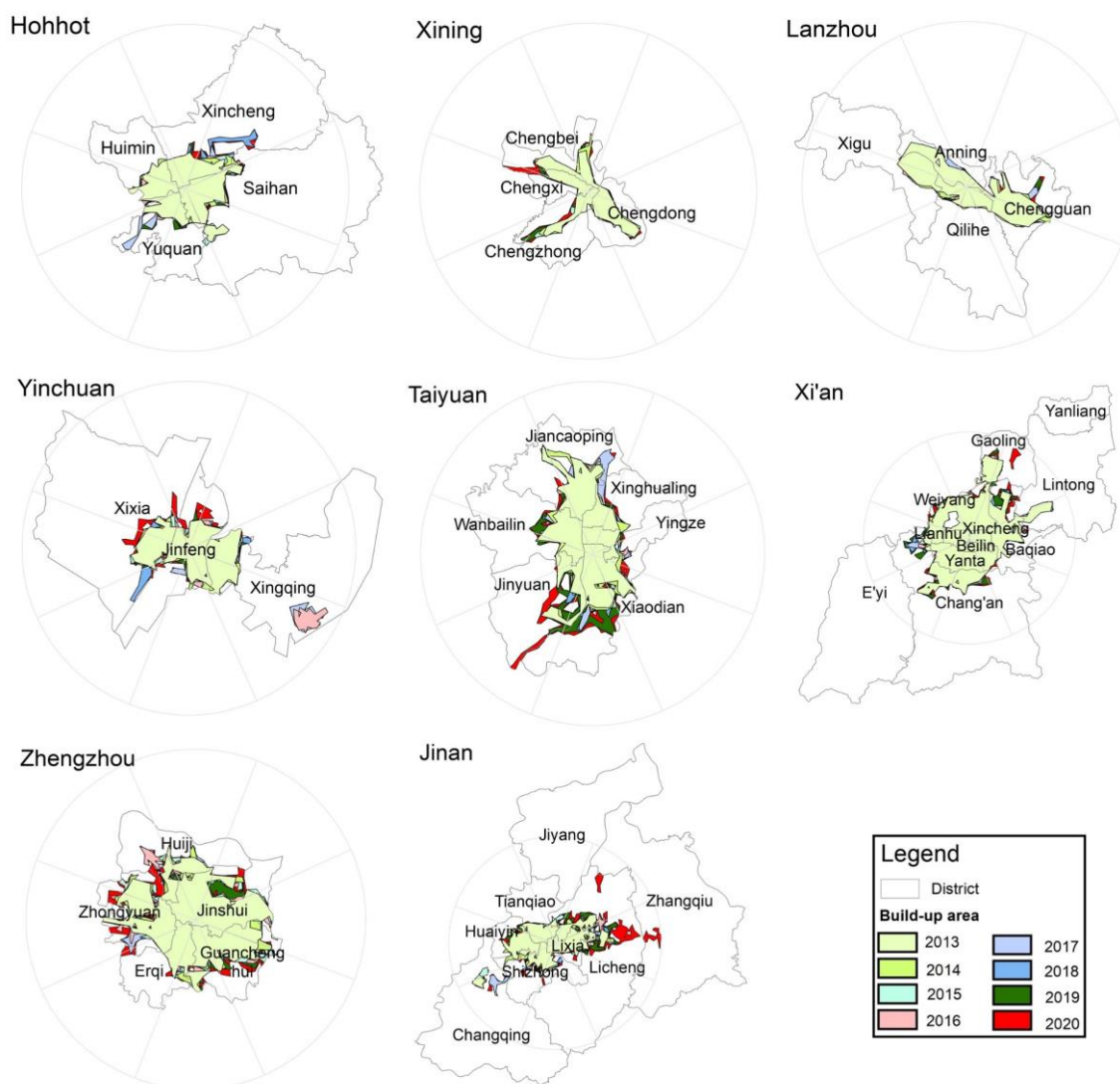


Figure 4. Spatial changes of urban built-up areas in the Yellow River Basin from 2013 to 2020.

Table 2. Built-up areas of provincial capitals extracted from NTL from 2013 to 2020.

	Time	Upper Reach				Middle Reach			Lower Reach
		Xining	Lanzhou	Yinchuan	Hohhot	Taiyuan	Xi'an	Zhengzhou	Jinan
AREA (km ²)	2013	115.31	195.05	201.02	217.28	312.38	786.96	442.89	310.81
	2020	141.17	187.66	269.22	246.70	457.38	883.71	568.11	513.47
Expansion rate <i>V</i> (km ² /year)	2013–2020	3.69	−1.06	9.74	4.20	20.72	13.82	17.89	28.95
Expansion intensity <i>N</i> (%)	2013–2020	3.20	−0.54	4.85	1.93	6.63	1.76	4.04	9.31

4.3. Spatial Expansion Characteristics of Urban Built-Up Areas

From 2013 to 2020, the built-up area in eight directions was evaluated to show the expansion direction of different cities' built-up areas (Figure 5). During the period 2013–2020, the urban area of Xining expanded primarily westwards and southwestwards around the east–west axis; the urban area of Lanzhou did not expand significantly during this period; the urban area of Yinchuan expanded northwards and westwards around the “southeast–northwest” axis; the urban area of Hohhot expanded noticeably in the northeast direction; the urban area of Taiyuan expanded significantly southwards and southwestwards mainly around the “east–west” axis, with a slight change in the built-up area in the northern area; Xi'an expanded on both sides of the “northwest–southeast” axis, with the largest expansion in the northeast and west directions; the built-up area of Jinan expanded mainly in the east and northeast regions, with a slow expansion in the southwest; the built-up area of Zhengzhou expanded outwards in a “pancake” pattern, with a larger area growth in the northwest and southeast directions.

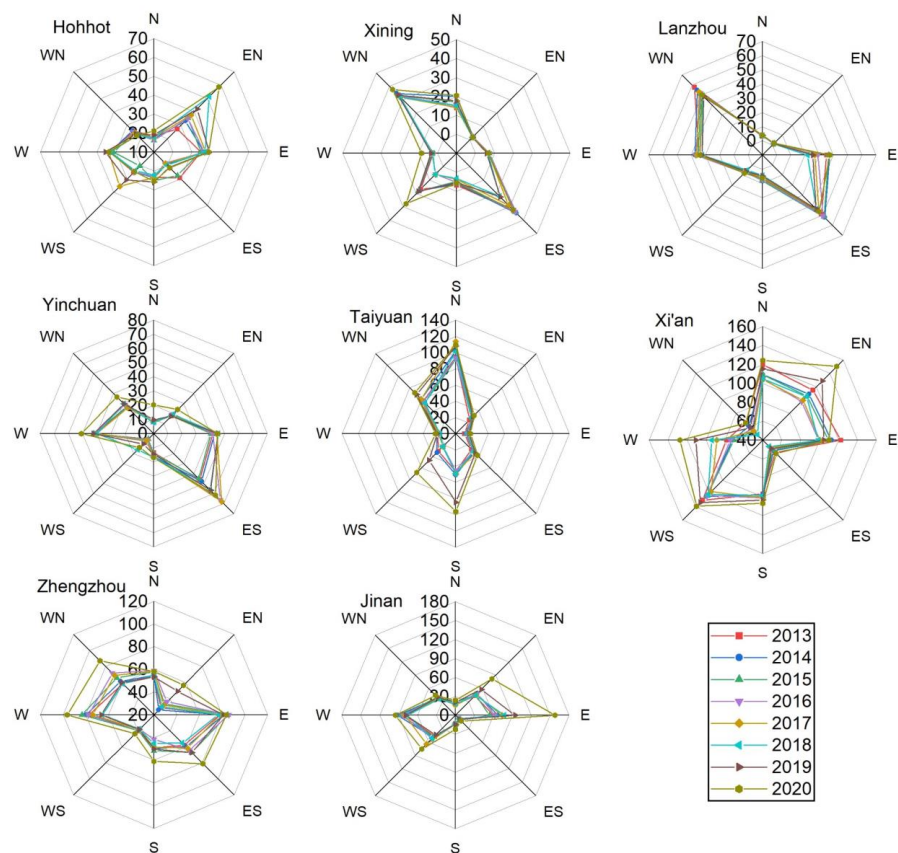


Figure 5. Spatial differentiation of urban built-up area expansion in the Yellow River Basin from 2013 to 2020.

4.4. Light Intensity Changes in Urban Built-Up Area Expansion

The capital cities of the Yellow River Basin are located along the upper, middle, and lower reaches of the river, with the built-up area steadily increasing from the upper to the lower reaches. Average nighttime light intensity (ANTL) and total nighttime light intensity (TNTL) data from urban built-up areas were divided into quadrants by upstream, middle, and downstream; they were studied to determine their correlation with urban built-up areas. The TNTL and the built-up area (AREA) had a significant positive correlation, with a correlation coefficient $R = 0.902$ (Figure 6). The ANTL was also positively correlated with AREA, but the correlation was weaker, with a correlation coefficient R of only 0.185.

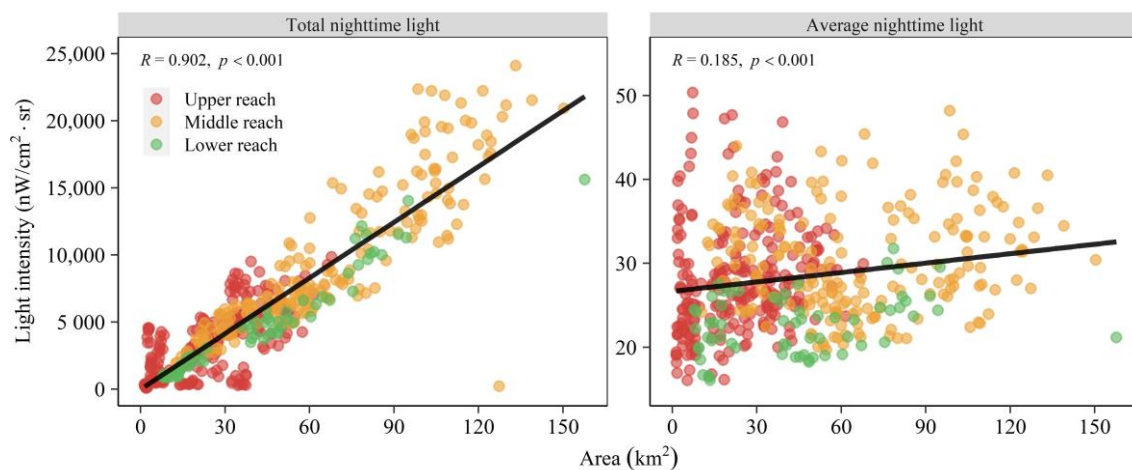


Figure 6. Correlation analysis of average nighttime light intensity (ANTL) and total nighttime light intensity (TNTL) and the built-up area in the upper, middle, and lower reaches of the Yellow River Basin.

The majority of built-up areas in the Yellow River Basin are in the middle and lower reaches, which likewise have higher overall light intensity; the places with the lowest total light intensity are generally found upstream. The built-up areas of cities in the upper, medium, and lower reaches revealed a lesser variation in terms of average light intensity. The greater the city's built-up area, the greater its ability to accommodate the population, and with the increase in population, the corresponding total light intensity is relatively high overall; however, due to the spatial distribution characteristics of the population and urban lights, the average light intensity per unit area of the built-up area is not closely correlated to the actual size of the built-up area.

4.5. Correlation between Urban Light Intensity and Human Activities

Urban expansion is represented not only in an increase in an urban area but also in an increase in the intensity of human activity in the cities. Changes in the intensity of human activity can be seen indirectly in socioeconomic parameters such as population and GDP. As a result, the correlation between urban light intensity (TNTL and ANTL) and socioeconomic indicators closely related to human activities, such as population and GDP in the Yellow River Basin, was examined to reflect the intensity of human activity and socioeconomic variations in each city's built-up areas during urban expansion.

From 2013 to 2019, the TNTL in built-up areas of cities in the Yellow River Basin showed a significant positive correlation with both GDP and population (Table 3), with the correlation between TNTL and population ($R = 0.8586$) being higher than the correlation between TNTL and GDP ($R = 0.7338$). The average light intensity ANTL was not connected with GDP or population in general ($R < 0.001$), but the ANTL of built-up regions of cities in various geographical areas was considerably and positively correlated with GDP and population, particularly in cities in the middle and lower reaches. The light intensity had a correlation coefficient of around 0.9 with both GDP and population in Jinan's built-up area,

whereas in Hohhot, the correlation coefficient R between light intensity and GDP was less than 0.2, but the correlation coefficient R between light intensity and the population was close to 0.9. The light intensity in the built-up region of Lanzhou is negatively correlated with GDP and population among the major cities in the entire Yellow River Basin. This demonstrates that the correlations between light intensity (TNTL and ANTL) and GDP and population in various Yellow River Basin cities are not consistent.

Table 3. Correlation analysis of TNTL and ANTL with GDP and population of urban built-up areas in the Yellow River Basin from 2013 to 2019.

City		Correlation Coefficient	GDP	Population
		(R)		
Upper reach	Hohhot	ANTL	0.1659	0.8927
		TNTL	0.1296	0.9003
	Xining	ANTL	0.9736	0.8765
		TNTL	0.5761	0.4578
	Lanzhou	ANTL	−0.4196	−0.5191
		TNTL	−0.8389	−0.8771
Yinchuan	ANTL	0.6753	0.5534	
	TNTL	0.7528	0.6310	
Middle reach	Taiyuan	ANTL	0.8716	0.6607
		TNTL	0.8270	0.8402
	Xi'an	ANTL	0.8610	0.8833
		TNTL	0.7263	0.7367
	Zhengzhou	ANTL	0.9163	0.9269
		TNTL	0.8919	0.8012
Lower reach	Jinan	ANTL	0.9358	0.8887
		TNTL	0.9588	0.9307

5. Discussion

5.1. Correlation between NTL and Human Activities in Urban Expansion

Many studies have found significant correlations between light intensity values influenced by NTL and social and economic indicators, and the use of NTL data allows spatialization of socioeconomic factors such as urban population and GDP to investigate the characteristics of uneven socioeconomic development at the regional scale [27,37–39]. The correlation analysis of light intensity and GDP and population of cities in the Yellow River Basin from 2013 to 2019 revealed that the correlation between NTL data and socioeconomic activity indicators differs by area, which is consistent with the previous study [40]. The more economically developed intermediate and downstream cities have greater commercial economic vitality and mature commercial spatial structures in built-up areas, demonstrating a stronger association between light intensity and human activities and social economy. Because the distribution of commercial spatial structure and service capacity within the metropolitan area of Jinan is the best among Yellow River Basin capital cities [41], the light intensity has a high and significant correlation with human activities and social economy in Jinan. In upstream, less economically developed cities, the correlation coefficients between light intensity and GDP and population are lower than that in middle and downstream cities.

Lanzhou, one of the upstream cities in the Yellow River Basin, had a negative relationship between light intensity and GDP, and population. Lanzhou's GDP and population increased from 2013 to 2019, yet the light intensity of the built-up region fell during the same period (Figure 7). Lanzhou's total light intensity has significantly fallen since 2014, and the maximum light intensity (MAXTL) in the built-up region has similarly shown a decreasing trend since 2013. According to an investigation, the train station is the geographic location with the highest light intensity in the built-up area. Lanzhou statistics from 2013 to 2019 demonstrate that the city's social economy was transitioning from conventional energy-consuming industries to high-tech businesses. In Lanzhou, the added value of high energy-consuming businesses such as thermal power generation, petroleum

industry, and petrochemical industry was gradually dropping, while investment in fields such as the electronics industry was gradually expanding. As a result, the nighttime light intensity in Lanzhou gradually decreased over five years. Thus, despite deviations from national statistical results, estimation results of socioeconomic indicators using NTL data can still be used as an observed variable to analyze socioeconomic progress under particular conditions [42–44].

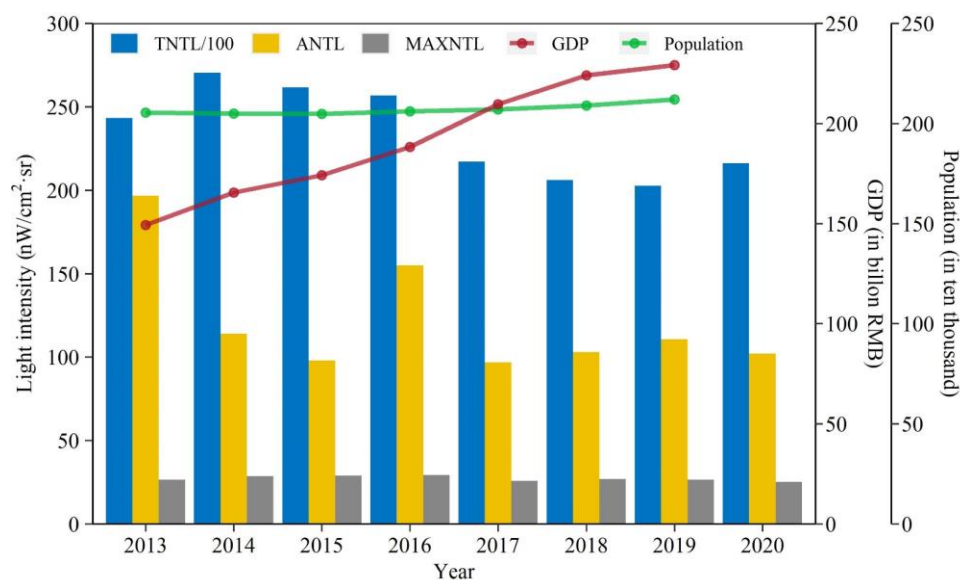


Figure 7. Changes in light intensity and GDP and population in Lanzhou from 2013 to 2019.

5.2. Natural Factor Constraints in the Urban Expansion of the Yellow River Basin

The natural geographical factors around the city not only provide the initial conditions for the formation and development but also play a restricting role in urban expansion. The Yellow River Basin comprises a broad west–east swath and the number of provincial capital cities diminishes from upstream to downstream, with elevation decreasing from 2237 m to 68 m [2]. Diverse spatial differentiation features were shaped throughout urban expansion as a result of the different geographical factors of each metropolis. The basin’s urban built-up area is inversely correlated to elevation and slope, with correlation coefficients of -0.5501 and -0.3515 , respectively. Although the cities expand outwards in different directions, they all have one thing in common: they all expand gradually outwards along with gently sloping regions. As a result, among the geographical elements, landform is a key factor restricting urban expansion [45,46].

The majority of the cities in the upper parts of the Yellow River Basin are located at higher altitudes (Table 1) and are surrounded by mountains; among them, Lanzhou and Xining have the highest altitudes and are more obviously influenced by topographical factors. The growth of GDP and the increase in urban population would undoubtedly cause the outward expansion of urban built-up regions in the process of socioeconomic development of cities; changing the terrain to allow human habitation will considerably increase the cost of urban expansion. As a result, cities in the Yellow River Basin’s upper reaches, which are more constrained by natural geographical elements, are less developed and expanded than those in the middle and lower reaches.

6. Conclusions

- (1) The Yellow River Basin’s NTL data can objectively depict the spatial and temporal dynamics of urban expansion in the basin. From 2013 to 2020, the built-up area of each province’s capital city in the Yellow River Basin steadily rose from upstream to downstream, with an increasing tendency over time. The cities in the upstream, middle, and downstream exhibit imbalanced urban development, with the upstream

cities having a smaller urban expansion area, expansion rate, and intensity than the middle and downstream cities. The natural geographical factors surrounding cities have a spatial influence on the urban expansion process, and each city's expansion has distinct spatial differentiation characteristics.

- (2) During the urbanization process, more developed middle and downstream cities have a significant positive correlation between light intensity, GDP, and population. The relationship between light intensity and GDP and population is weaker in upstream cities. During the development of cities in the Yellow River Basin's middle and lower reaches, their built-up areas shaped a well-developed commercial economic structure and a high degree of coordination with the spatial pattern of human flow distribution, and light data can well demonstrate GDP and population development changes. The cities in the upper Yellow River Basin are constrained by their natural geographical environment; their urban development is slower than that of the cities in the middle and lower reaches, and the commercial structure within the cities must be adjusted to promote urban economic development and to accommodate population growth caused by urban development.

Author Contributions: J.W., S.Q. and S.M. conceived and designed the experiments; C.W., J.D. and F.T. processed the data and made suggestions for revision; Y.L. and J.W. designed the workflow and edited the code with JavaScript; S.M. and J.W. analyzed the data and drew the pictures; J.W. wrote the paper. All authors have read and agreed to the published version of the manuscript.

Funding: This research was funded by Science and Technology Project of Henan Province (212102310024) and Talents Training Program of Henan Academy of Sciences (220401010) and Special Project for Team Building of Henan Academy of Sciences, grant number (200501007), and the projects of the central government to guide local scientific and technological development (211201004).

Institutional Review Board Statement: Not applicable.

Informed Consent Statement: Not applicable.

Data Availability Statement: Not applicable.

Conflicts of Interest: The authors declare no conflict of interest.

References

1. Wei, H.J.; Xue, D.; Huang, J.C.; Liu, M.X.; Li, L. Identification of coupling relationship between ecosystem services and urbanization for supporting ecological management: A case study on areas along the Yellow River of Henan province. *Remote Sens.* **2022**, *14*, 2277. [[CrossRef](#)]
2. Zhang, X.L.; Kong, Y.S.; Ding, X.H. How High-quality urbanization affects utilization efficiency of agricultural water resources in the Yellow River Basin under double control action? *Sustainability* **2020**, *12*, 2869. [[CrossRef](#)]
3. Lyu, R.F.; Zhang, J.M.; Xu, M.Q.; Li, J.J. Impacts of urbanization on ecosystem services and their temporal relations: A case study in Northern Ningxia, China. *Land Use Policy* **2018**, *77*, 163–173. [[CrossRef](#)]
4. Qiao, R.; Li, H.M.; Han, H. Spatio-Temporal coupling coordination analysis between urbanization and water resource carrying capacity of the provinces in the Yellow River Basin, China. *Water* **2021**, *13*, 376. [[CrossRef](#)]
5. Xing, L.; Xue, M.G.; Hu, M.S. Dynamic simulation and assessment of the coupling coordination degree of the economy-resource-environment system: Case of Wuhan City in China. *J. Environ. Manag.* **2019**, *230*, 474–487. [[CrossRef](#)]
6. Shi, L.P.; Cai, Z.Y.; Ding, X.H.; Di, R.; Xiao, Q.Q. What factors affect the level of green urbanization in the Yellow River Basin in the context of new-type urbanization? *Sustainability* **2020**, *12*, 2488. [[CrossRef](#)]
7. Du, X.; Meng, Y.; Fang, C.; Li, C. Spatio-temporal characteristics of coupling coordination development between urbanization and Shandong Peninsula urban agglomeration. *Acta Ecol. Sin.* **2020**, *40*, 5546–5559. (In Chinese)
8. Yue, W.Z.; Gao, J.B.; Yang, X.C. Estimation of gross domestic product using multi-sensor remote sensing data: A case study in Zhejiang province, East China. *Remote Sens.* **2014**, *6*, 7260–7275. [[CrossRef](#)]
9. Zheng, Q.M.; Weng, Q.H.; Wang, K. Characterizing urban land changes of 30 global megacities using nighttime light time series stacks. *ISPRS J. Photogramm. Remote Sens.* **2021**, *173*, 10–23. [[CrossRef](#)]
10. Levin, N.; Kyba, C.C.M.; Zhang, Q.L.; de Miguel, A.S.; Roman, M.O.; Li, X.; Portnov, B.A.; Molthan, A.L.; Jechow, A.; Miller, S.D.; et al. Remote sensing of night lights: A review and an outlook for the future. *Remote Sens. Environ.* **2020**, *237*, 111443–111476. [[CrossRef](#)]

11. Hu, X.F.; Qian, Y.G.; Pickett, T.A.S.; Zhou, W.Q. Urban mapping needs up-to-date approaches to provide diverse perspectives of current urbanization: A novel attempt to map urban areas with nighttime light data. *Landsc. Urban Plan.* **2020**, *195*, 103079–103095. [[CrossRef](#)]
12. Shi, K.F.; Huang, C.; Yu, B.L.; Yin, B.; Huang, Y.X.; Wu, J.P. Evaluation of NPP-VIIRS night-time light composite data for extracting built-up urban areas. *Remote Sens. Lett.* **2014**, *5*, 358–366. [[CrossRef](#)]
13. Milesi, C.; Elvidge, C.D.; Nemani, R.R.; Running, S.W. Assessing the impact of urban land development on net primary productivity in the southeastern United States. *Remote Sens. Environ.* **2003**, *86*, 401–410. [[CrossRef](#)]
14. Zhou, Y.; Li, C.G.; Zheng, W.S.; Rong, Y.F.; Liu, W. Identification of urban shrinkage using NPP-VIIRS nighttime light data at the county level in China. *Cities* **2021**, *118*, 103373–103383. [[CrossRef](#)]
15. Su, Y.X.; Chen, X.Z.; Wang, C.Y.; Zhang, H.G.; Liao, J.S.; Ye, Y.Y.; Wang, C.J. A new method for extracting built-up urban areas using DMSF-OLS nighttime stable lights: A case study in the Pearl River Delta, southern China. *GISci. Remote Sens.* **2015**, *52*, 218–238. [[CrossRef](#)]
16. Shi, K.F.; Yu, B.L.; Hu, Y.J.; Huang, C.; Chen, Y.; Huang, Y.X.; Chen, Z.Q.; Wu, J.P. 2015 Modeling and mapping total freight traffic in China using NPP-VIIRS nighttime light composite data. *GISci. Remote Sens.* **2015**, *52*, 274–289. [[CrossRef](#)]
17. Xu, H.M.; Hu, S.G. Chinese city size evolution under perspective of nighttime light remote sensing. *Geomat. Inform. Sci. Wuhan Univ.* **2021**, *46*, 40–49. (In Chinese)
18. Hu, Y.F.; Zhao, G.H.; Zhang, Q.L. Spatial distribution of population data based on nighttime light and LUC data in the SichuanChongqing region. *J. Geo-Inf. Sci.* **2018**, *20*, 68–78. (In Chinese)
19. Henderson, J.V.; Storeygard, A.; Weil, D.N. Measuring economic growth from outer space. *Am. Econ. Rev.* **2012**, *102*, 994–1028. [[CrossRef](#)]
20. Feng, Z.; Peng, J.; Wu, J.S. Using DMSF/OLS nighttime light data and K-means method to identify urban-rural fringe of megacities. *Habitat Int.* **2020**, *103*, 10227–10238. [[CrossRef](#)]
21. Liu, Q.P.; Yang, Y.C.; Fu, D.X.; Li, H.Y.; Tian, H.Z. Urban spatial expansion based on DMSF_OLS nighttime light data in China in 1992–2010. *Sci. Geogr. Sin.* **2014**, *34*, 129–136. (In Chinese)
22. Chen, Z.Q.; Yu, B.L.; Song, W.; Liu, H.X.; Wu, Q.S.; Shi, K.F.; Wu, J.P. A new approach for detecting urban centers and their spatial structure with nighttime light remote sensing. *IEEE Trans. Geosci. Remote Sens.* **2017**, *55*, 6305–6319. [[CrossRef](#)]
23. Yu, B.L.; Tang, M.; Wu, Q.S.; Yang, C.S.; Deng, S.Q.; Shi, K.F.; Chen, P.; Wu, J.P.; Chen, Z.Q. Urban Built-Up Area Extraction From Log-Transformed NPP-VIIRS Nighttime Light Composite Data. *IEEE Geosci. Remote Sens. Lett.* **2018**, *15*, 1279–1283. [[CrossRef](#)]
24. Peng, J.; Hu, Y.N.; Liu, Y.X.; Ma, J.; Zhao, S.Q. A new approach for urban-rural fringe identification: Integrating impervious surface area and spatial continuous wavelet transform. *Landsc. Urban Plan.* **2018**, *175*, 72–79. [[CrossRef](#)]
25. Ma, T. Multi-level relationships between satellite-derived nighttime lighting signals and social media-derived human population dynamics. *Remote Sens.* **2018**, *10*, 1128. [[CrossRef](#)]
26. Zhao, M.; Cheng, W.M.; Zhou, C.H.; Li, M.C.; Wang, N.; Liu, Q.Y. GDP spatialization and economic differences in south China based on NPP-VIIRS nighttime light imagery. *Remote Sens.* **2017**, *9*, 673. [[CrossRef](#)]
27. Li, K.N.; Chen, Y.H.; Li, Y. The random forest-based method of fine-resolution population spatialization by using the international space station nighttime photography and social sensing data. *Remote Sens.* **2018**, *10*, 1650. [[CrossRef](#)]
28. Li, Y.L.; Cheng, G.; Yang, J.; Yuan, D.F. Refined spatial simulation of regional economy based on nighttime lighting data from remote sensing: A case study of Henan province. *Areal Res. Dev.* **2020**, *39*, 41–47. (In Chinese)
29. Liang, H.D.; Guo, Z.Y.; Wu, J.P.; Chen, Z.Q. GDP spatialization in Ningbo city based on NPP/VIIRS night-time light and auxiliary data using random forest regression. *Adv. Space Res.* **2020**, *65*, 481–493. [[CrossRef](#)]
30. Mellander, C.; Lobo, J.; Stolarick, K.; Matheson, Z. Night-time light data: A good proxy measure for economic activity? *PLoS ONE* **2015**, *10*, 139779–139797. [[CrossRef](#)]
31. Gorelick, N.; Hancher, M.; Dixon, M.; Ilyushchenko, S.; Thau, D.; Moore, R. Google Earth Engine: Planetary-scale geospatial analysis for everyone. *Remote Sens. Environ.* **2017**, *202*, 18–27. [[CrossRef](#)]
32. Goldblatt, R.; You, W.; Hanson, G.; Khandelwal, A. Detecting the boundaries of urban areas in India: A dataset for pixel-based image classification in Google Earth Engine. *Remote Sens.* **2016**, *8*, 634. [[CrossRef](#)]
33. Kumar, L.; Mutanga, O. Google Earth Engine applications since inception: Usage, trends, and potential. *Remote Sens.* **2018**, *10*, 1509. [[CrossRef](#)]
34. Gong, P.; Chen, B.; Li, X.C.; Liu, H.; Wang, J.; Bai, Y.Q.; Chen, J.M.; Chen, X.; Fang, L.; Feng, S.L.; et al. Mapping essential urban land use categories in China (EULUC-China): Preliminary results for 2018. *Sci. Bull.* **2020**, *65*, 182–187. [[CrossRef](#)]
35. Chen, J.; Liao, A.P.; Chen, J.; Peng, S.; Chen, L.J.; Zhang, H.W. 30-meter global land cover data product- GlobeLand30. *Geomat. World* **2017**, *24*, 1–8.
36. Otsu, N.A. Threshold selection method from gray-level histograms. *IEEE Trans. Syst. Man Cybern.* **2007**, *9*, 62–66. [[CrossRef](#)]
37. Bennett, M.M.; Smith, C.L. Advances in using multitemporal night-time lights satellite imagery to detect, estimate, and monitor socioeconomic dynamics. *Remote Sens. Environ.* **2017**, *192*, 176–197. [[CrossRef](#)]
38. Shi, K.F.; Yu, B.L.; Huang, Y.X.; Hu, Y.J.; Yin, B.; Chen, Z.Q.; Chen, L.J.; Wu, J.P. Evaluating the ability of NPP-VIIRS nighttime light data to estimate the gross domestic product and the electric power consumption of China at multiple scales: A comparison with DMSF-OLS data. *Remote Sens.* **2014**, *6*, 1705–1724. [[CrossRef](#)]

39. Li, F.; Zhang, X.B.; Gu, S.B.; Qian, A. Capability assessment of DMSP-OLS and NPP-VIRS nighttime light data estimating statistical indicators: A case of county-level GDP, population and energy consumption in Beijing-Tianjin-Hebei region. *Bull. Surv. Mapp.* **2020**, *9*, 89–93. (In Chinese)
40. He, C.Y.; Shi, P.J.; Li, J.G.; Chen, J.; Pan, Y.Z.; Li, J. Reconstruction of Chinese mainland city spatial process in 1990s based on DMSP/OLS night lighting data and statistics. *Chin. Sci. Bull.* **2006**, *51*, 856–861. (In Chinese)
41. Ye, Q.; Zhao, Y.; Tan, C.; Ma, M.Y.; Chen, N. Research on commercial spatial structure and spatial service capability of provincial capital cities along the Yellow River in the new period. *J. Nat. Resour.* **2021**, *36*, 103–113. (In Chinese) [[CrossRef](#)]
42. Berliant, M.; Weiss, A. Measuring economic growth from outer space: A comment. *MPRA Pap.* **2013**, *102*, 994–1028.
43. Yang, M.; Wang, S.X.; Zhou, Y.; Wang, L.T. Review on applications of DMSP/OLS night-time emissions data. *Remote Sens. Technol. Appl.* **2011**, *26*, 45–51. (In Chinese)
44. Xu, K.N.; Chen, F.L.; Liu, X.Y. The Truth of china economic growth: Evidence from global night-time light data. *Econ. Res. J.* **2015**, *9*, 17–29. (In Chinese)
45. Zhou, Y.; Xie, B.P.; Zhao, H.Y.; Chen, Y.; Pei, T.T.; Liu, S.Q. Study on Spatial-temporal Pattern and Dynamic Evolution of City Scale at County Level in China Based on Night-time Light Data. *Resour. Environ. Yangtze Basin* **2019**, *28*, 250–261. (In Chinese)
46. Wen, T.Z.; Qiang, W.; Liu, X.J. Exploring the geography of urban comprehensive development in mainland Chinese cities. *Land Use Policy* **2022**, *115*, 106004–106013. [[CrossRef](#)]